Computational Screening of Phytochemicals present in some Nigeria Medicinal Plants against Sickle Cell Disease

Yemisi Elizabeth Asibor
yemisi.asibor@uniosun.edu.ng
Osun State University
Dayo Felix LATONA
Osun State University
Abel Kolawole OYEBAMIJI
Bowen University
Banjo SEMIRE
Ladoke Akintola University of Technology

Article

Keywords: Sickle Cell Diseases, Bioactive compounds, PASS, ADMET, DFT, Molecular docking, dynamic simulation

Posted Date: August 21st, 2024

DOI: https://doi.org/10.21203/rs.3.rs-4691722/v1

Additional Declarations: No competing interests reported.

Version of Record: A version of this preprint was published at Scientific Reports on November 1st, 2024. See the published version at https://doi.org/10.1038/s41598-024-75078-w.

Abstract

Four hundred Phytochemical (bio-active) compounds having predictive activity for treating Sickle Cell Anemia were screened, using PASS online computational resource. Twenty-six compounds out of the four hundred compounds which showed high probability for treating sickle were further screened for pharmacokinetics profiles (ADMET properties) using SwissAdmet, AdmetSAR 2 and Pro-tox II online resources. Only thirteen compounds that displayed good ADMET properties from the twenty -six were further used for DFT calculations and molecular docking against carbonmonoxy sickle hemoglobin (PDB ID: 5E6E). Molecular docking analysis reinforced by DFT calculations showed that two compounds, phenanthrene-5,6-dione **(A9)** and 2-(3,4-dihydroxyphenyl)-5,7-dihydroxychromen-4-one **(A13, Luteolin)** have the best binding affinity of -8.3 and − 8.9 kcal/mol, respectively, compared to voxelotor (GBT-440), a drug use in treating sickle cell disease. Molecular dynamic simulations showed that 2-(3,4-dihydroxyphenyl)-5,7-dihydroxychromen-4-one **(A13, Luteolin)** is highly stable with the protein than voxelotor.

Introduction

When considering the spectrum of genetic disorders and diseases that impart humanity, only a few can match the multifaceted challenges posed by sickle cell diseases (SCD) and related disorders. Sickle cell disease is a potentially devastating condition resulting from an autosomal recessive inherited hemoglobinopathy. It is a global sickness that transcends national and ethnic boundaries, affecting diverse population worldwide. The molecular basis of sickle cell disease lies in a single base mutation, specifically adenine to thymine, resulting in the substitution of valine for glutamine acid at the sixth codon of the β-globin chain (βS), this leads to high level of 2,3-diphosphoglycerate (2,3-DPG) which interacted with hemoglobin to reduce HbS solubility and promotes polymerization [1]. This substitution, in which a polar glutamic acid residue is replaced by a non-polar valine molecule, leads to the formation of a sticky region on the β-globin chain [2]. Sickle Cell Disease (SCD) is characterized by a significant burden of illness and a decreased life expectancy primarily attributable to hemolytic anemia and vaso-occlusive processes.

These processes give rise to painful vaso-occlusive episodes, often necessitating hospitalization and contributing to the development of chronic organ damage. Additional complications associated with SCD exhibit considerable variability among individuals, encompassing both acute and chronic issues such as stroke, acute chest syndrome, retinopathy, renal disease, osteonecrosis, cardiovascular problems, and leg ulcers [3, 4]. In spite of its significance in the realm of public health, there are only two recently approved drugs by the FDA, namely voxelotor and crizanlizumab [5, 6] hence the use of medicinal plants as alternative and affordable medicine for the treatment of this disease.

Phytochemicals are chemical compounds naturally produced as part of a plant's metabolic processes. These substances are commonly referred to as "secondary metabolites" and encompass several categories, such as alkaloids, flavonoids, coumarins, glycosides, gums, polysaccharides, phenols, tannins, terpenes, and terpenoids [7, 8]. These phytochemicals can be found in a wide array of plants that hold significant importance in both human and animal diets, including fruits, seeds, herbs, and vegetables [9]. Many of these phytochemical constituents are potent bioactive compounds found in various parts of medicinal plants, serving as precursors for the synthesis of valuable drugs [10]. Several medicinal plants native to Nigeria have been reported to have potential efficacy in the treatment of sickle cell disease [11].

These plants include *Eugenia caryophyllata* (clove, known as "kanunfari" in Hausa), *Piper guineense* (referred to as "eche" in Idoma or "akwa-ose" in Igbo), grains of paradise (*Aframomum melegueta*, locally known as "otuta" in Idoma), *Sorghum bicolor* (notably, the leaf stalk yields an extract resembling blood), and *Pterocarpus osun*, abundant in Osun state, western region of Nigeria [12–14]. These plants are utilized for various health conditions, including the management of sickle cell anemia. They are major herbal components in the traditional Yoruba recipe that forms the basis for the antisickling drug Niprisan [15].

Density Functional Theory (DFT) is a computational chemistry method that has surged in popularity in recent times for its precise computation of molecular properties. DFT has been widely employed to calculate the electronic structure and attributes of molecules in various states, encompassing both ground and excited electronic configurations, across diverse environments [16, 17]. It serves as a formidable instrument for scrutinizing the unchanging aspects of electronic systems, such as their geometrical arrangements and relative energy levels [18–19].

Prediction of Activity Spectra for Substances (PASS), an online web server (http://www.pharm a expe rt.ru/passonline) predicts over 3500 kinds of biological activity, this biological activity includes including pharmacological effects, mechanisms of action, toxic and adverse effects, interaction with metabolic enzymes and transporters influence on gene expression [20]. Absorption, Distribution, Metabolism, Excretion and Toxicity (ADMET) is an important aspect or stage of drug discovery. It evaluates the safety of the drug candidates. ADMET is very crucial because undesirable pharmacokinetics and toxicity of candidate compounds are the main reason for the failure of drug development. Thus, Prediction of Activity Spectra for Substances (PASS), Absorption, Distribution, Metabolism, Excretion and Toxicity (ADMET), Density Functional Theory (DFT), molecular docking and molecular dynamic simulation would be used in assessing the potency of selected phytochemicals against sickle cell disease.

Therefore, the main objective of this work is computationally screening some bio-active compounds from medicinal plants (*Eugenia caryophyllata, Piper guineense, Aframomum melegueta*, *Sorghum bicolor* and *Pterocarpus osun*) that possesses therapeutic applications in managing sickle cell disease with targeted carbonmoxy sickle hemoglobin in R state conformation (PBD: 5E6E), the polymerization of deoxygenated (T-state) sickle hemoglobin (Hb S) into fibers that distort red blood cells, through PASS, ADMET, DFT, molecular docking and molecular dynamic simulation.

Materials and Methods

The canonical smiles of four hundred (400) bioactive compounds were downloaded and save from PubChem database. The canonical smiles of bioactive compounds obtained were subjected to prediction of activity spectra of substances (PASS) web server (www.https:/pharmaexpert.ru.passonline/) [21] to know if these compounds can actually treat sickle cell diseases. The compounds that showed probability to be active for treating sickle diseases was subjected to Absorption, Distribution, Metabolism, Excretion and Toxicity (ADMET) and Prediction Toxicity of chemical compounds using Pro-Tox II software. This was evaluated using two ADMET webserves namely SwissADMET (http://lmmd.ecust.edu.cn/admetsar2/result/?tid=684417) and ADMET Sar.2.0 (www.admetexp.org) [22, 23]. The Oral bioavailability assessments of the compounds were done using the SwissADME web server (http://www.swissadme.ch/) [24]. The molecular descriptors which describe the anti-sickle activities of the studied compounds evaluated from the optimized structure of the phytochemicals from DFT calculations. DFT with Becke's three parameter hybrid functional with correlation of Lee, Yang and Parr (B3LYP) was used [25, 26] with 6–31 + G(d,p) basis set was used for the optimization as implemented in Spartan 14 quantum chemistry software [27].

Preparation of the ligands

The sickle cell disease inhibitory activities of thirteen selected ligands (A1-A13) that have high probability, less toxicity and good ADMET properties from different natural plants database was studied against the protein in hemoglobin S (carbonmonoxy sickle hemoglobin PDB ID: 5E6E, resolution 1.76Å), while Voxelotor (GBT-440) as used as standard drug for treating SCD. The 3D SDF conformer of all the ligands and standard drug were downloaded from PubChem Database (https://pubchem.ncbi.nlm.nih.gov).

Preparation of Target protein

The crystal structures of the protein carbonmonoxy sickle hemoglobin (PDB ID: 5E6E) was downloaded in PDB format from the protein data bank (http://www.rcsb.org/pdb), Fig. 1, with a resolution of retrieved structure as 1.76Å. All water molecules, heteroatoms and unwanted complexes were removed from the crystal structure of the downloaded protein; this was done to ensure that undesired molecular interactions and impurities are avoided, and that no molecules interfered with the potential binding sites of the target proteins during molecular docking. This was done using Discovery Studio Software v.2020. The Ramachandran plot revealed that the receptor was of good quality by using the Volume, Area, Dihedral Angle Reporter (VADAR) webserver.

Structural and active site analysis of Crystal Structure of Carbonmonoxy Sickle Hemoglobin in R-State Conformation (PDB ID: 5E6E)

The X-ray crystallographic structure of the Crystal Structure of Carbonmonoxy Sickle Hemoglobin in R-State Conformation (PDB ID: 5E6E) as shown in Fig. 1a contains 136 amino acids residue complexed with protoporphyrin IX containing Fe. The Ramachandran plot of the protein reveals that the protein is viable for use (Fig. 1b). The resolution of the protases as revealed by X-ray diffraction was 1.76Å, crystal dimension is a = 53.352 Å, b = 53.352 Å, and c = 191.068 Å, with angles α (90.00), β (90.00) and Y (90.00), The R – values (free and work) are 0.243 and 0.193 while the total accessible surface area (TASA) on the protein is 432.6 Å. The final structure contains a dimer (α1β1) in the asymmetric unit, comprising 141 residues in the α-subunit, 146 residues in the β-subunit, 2 heme groups, 2 CO-ligated heme ligands, 2 toluene molecules, a phosphate molecule, and 442 water molecules. Carbonmonoxy Sickle Hemoglobin in R-State Conformation is useful in nitric oxide transport, oxygen transport, blood vessel diameter maintenance, scavenging of heme from plasma and regulation of blood pressure. The active sites in 5E6E are His A 58, Phe A 43, LeuA 29, LeuA 101 and ValA 62 [28, 29]. This binding pocket, ligand interactions, and all amino acids residues in the active sites of 5E6E, were established using the Computed Atlas for Surface Topography of Proteins (CASTp) (http://sts.bioe.uic.edu/castp/index .html? 2011) [30] and Biovia Discovery Studio (2019).

Molecular docking

Molecular docking and binding affinity scores of the optimized ligands and the standard drug against carbonmonoxy sickle hemoglobin (PDB ID: 5E6E) were performed using PxRy and Discovery studio software. The receptor (PDB ID: 5E6E) binding site center and dimension in x, y and z directions generated grid were 35.9837, 31.6925 and 59.0081 for center and 80.5073, 66.1331 and 25.0000 for dimension. The inhibition constant (Ki) μM of the ligands and the standard drug were calculated by employing their binding affinities (ΔG) kcal/mol as showed in (equations 1and 2), where R is gas constant, T = 298.15K (absolute temperature), K_i is the inhibition constant and ΔG is the binding energy.

$$\Delta G = -nRT \ln K_{eq} \quad (1)$$

$$K_i = \frac{1}{K_{eq}} \quad (2)$$

Molecular Dynamic Simulation

The Molecular Dynamic Simulations was performed for 100 (ns) simulation using GROningen MAchine for Chemical Simulations (GROMACS) tool 2018 version developed by the University of Groningen, Netherlands [31]. Pdb2gmx module was used to generate the required Carbonmonoxy Sickle Hemoglobin in R-State Conformation (PDB:5E6E) topology file followed by CHARMM36 all-atom force-field selection. phenanthrene-5,6-dione (A9), 2-(3,4-dihydroxyphenyl)-5,7-dihydroxychromen-4-one (A13) topology files were prepared and downloaded from the SwissParam server [32]. A triclinic-shaped water molecules-filled solvation unit cell was built. Addition of Na^+ and Cl^- ions was done for stabilization of the system followed by energy minimization. Equilibrium setup of the receptor (PDB: 5E6E) complex required and it was done followed by two-step ensembles NVT (constant number of particles, pressure, and temperature) and NPT (constant number of particles, pressure, temperature) [33]. All necessary ensembles deliver control over temperature, pressure coupling provides steadfastness and stabilization of the system during the whole simulation [34]. GORMACS have many inbuilt packages, for the receptor complex Molecular Dynamic Simulations analysis, gmx rms was utilized for Root Mean Square Deviation (RMSD) [35], gmx rmsf for Root Mean Square fluctuation (RMSF), gmx gyrate for the complete assessment of Radius of Gyration (Rg) [36] and gmx hydrogen bond for the calculation of numbers of hydrogen-bond (Hbond) formed during the interaction. Lastly, after 100ns molecular dynamic simulations, output trajectory files analyzed and graph plots were generated using Xmgrace program [37].

Results and Discussion

Prediction of Activity Spectra of Substances Database (PASS) for Biological activity of the ligands used in Treating SCD.

The canonical smiles of four hundred (400) bioactive compounds downloaded from PubChem database were subjected to prediction of activity spectra of substances (PASS) web server (www.https:/pharmaexpert.ru.passonline/) [21] to predict probable anti-sickle cell disease activity of the compounds. Out of the four hundred bio-active compounds, twenty-six compounds (26) showed probability to be active for treating sickle cell diseases as shown in Table 1 along with the standard drug, **Voxelotor (GBT-440)**, and thirteen these compounds with very good ADMET properties are in parenthesis: Zanthoxytol **(0.161 A1)**, Zingerone **(0.289, A2)**, Resveratrol **(0.242, A3)**, Scopoletin **(0.229 A4)**, Psoralin, 5-hydroxy **(0.214 A5)**, Isopsoralin **(0.194 A6)**, Pterostilbene **(0.238 A7)**, Phenoxethin **(0.191 A8)**, Phenanthroline-5,6-dione **(0.326 A9)**, Oxyresveratrol **(0.235 A10)**, M-Coumaric acid **(0.236 A11)**, Maesopsin **(0.177 A12)** and Luteolin **(0.182 A13).** The best three bio-active ligands from the predicted biological activity spectra are in the order: phenanthroline-9,10-dione (0.326) > (4-(4-hydroxy-3-methoxyphenyl) butan-2-one (zingerone, 0.289) > ((E)-3-(3-hydroxyphenyl)prop-2-enoic acid (M-coumaric acid, 0.236). The standard drug, voxelotor (GBT-440) has probability to be an active against sickle cell as 0.155, suggesting that all the thirteen bioactive compounds investigated have higher probabilities than the standard drug. Although, Palmitic acid (0.341), Pentadecanoic acid (0.341), Protocatechuic acid (0.433), Serine (0.308), Phenanthren-9-ol (0.319), Piperazine (0.249), Phenoxathin (0.216), P-Cymene (0.201) and Coumaric acid (0.216) showed higher probability of activity for treating sickle cell than the phenanthroline-9,10-dione, 4-(4-hydroxy-3-methoxyphenyl) butan-2-one and (E)-3-(3-hydroxyphenyl)prop-2-enoic acid compounds, but these compounds failed ADMET rules.

Table 1
PASS screening of the bio-active compounds and the standard drug for Sickle Cell.

S /N	Ligands	Probability to be active (Pa)	Probability to be inactive (Pi)
1.	Xylitol	0.183	0.087
2.	Zanthoxylol (A1)	0.161	0.121
3.	Zingerone (A2)	0. 289	0.017
4.	Resveratrol(A3)	0.242	0.036
5.	Scopoletin(A4)	0.229	0.043
6.	Serine	0.308	0.013
7.	Protocatechuic acid"	0.433	0.004
8.	Psoralin, 5-hydroxy-" (A5)	0.214	0.045
9.	Psoralin, n-decanoyl-5-oxo	0.180	0.022
10.	Isopsoralin (A6)	0.194	0.074
11.	Pterostilbene (A7)	0.238	0.038
12.	Piperazine	0.249	0.032
13.	Phenoxazine	0.216	0.053
14.	Phenoxathiin (A8)	0.191	0.077
15.	Phenanthrene	0.320	0.010
16.	Phenanthren-9-ol	0.319	0.010
17.	Phenanthrene-5,6-dione (A9)	0.326	0.009
18.	Pentadecanoic acid	0.341	0.008
19.	Nobilen	0.272	0.022
20.	o-Coumaric acid lactone	0.216	0.053
21.	Palmitic acid"	0.341	0.008
22.	P-cymene	0.201	0.066
23.	Oxyresveratrol (A10)	0.235	0.039
24.	M-coumaric acid"(A11)	0.236	0.039
25.	Maesopsin(A12)	0.177	0.095
26.	Luteolin (A13)	0.182	0.089
27.	Voxelotor (GBT-440) SD	0.155	0.131

- Physiochemical and ADMET properties

Twenty- six compounds with probability of activity for treating sickle cell, as well as voxelotor (GBT-440) drug were subjected to two ADMET profiling using online SwissADMET and ADMET Sar.2.0 [22]. SwissADME website was used to compute physicochemical descriptors as well as to predict ADMET parameters such as pharmacokinetic properties, synthetic accessibility, bioavailability score, Veber, Egan, Ghose, druglike nature, medicinal chemistry, water solubility, lipophility [38]. The druglikenss of the twenty-six ligands were estimated using Lipinski's rules of five, Veber filter, Egan filter, Ghose filter, Muggen filter and bioavailability score. The Lipinski filter or Lipinski's rule of five (Ro5) is the pioneer rule of five that characterizes small molecules based on physicochemical property profiles which includes hydrogen bond donor (HBD $\leq$ 5), hydrogen bond acceptor (HBA $\leq$ 10), molecular weight (150 $\leq$ MW $\leq$ 500), lipophilicity (log P $\leq$ 5) and ROTBs $\leq$ 10 [39, 40]. From the twenty-six compounds, thirteen ligands obeys the Lipinski's rule for hydrogen bond donor < 5, hydrogen bond acceptor < 10 and molecular weight from 150 -500g/mol, TPSA value $\leq$ 131.6 Å and WLogP value is $\leq$ 5.88 as displayed in Table 2. All have bioactivity score of 0.55 except M-coumaric acid" with bioactivity score of 0.85. It is evident that the thirteen ligands exhibited high gastrointestinal (GI) tract absorption which makes the ligands suitable as potential drug candidates. The BBB revealed that 2-(3,4-dihydroxyphenyl)-5,7-dihydroxychromen-4-one (A13), 2,4,6-trihydroxy-2-[(4-hydroxyphenyl) methyl]-1-benzofuran-3-one (A12) and 4-[(E)-2-(3,5-dihydroxyphenyl)ethenyl]benzene-1,3-diol (A10) may be able

to penetrate blood-brain barrier, this means that the above ligands will have no side effects on the central nervous system (CNS), whereas others including Voxelotor (GBT-440) showed penetration to blood-brain barrier (BBB) which may cause side effects to the central nervous system (CNS) [41].

The most important task of P-glycoprotein (P-gp) is to keep the central nervous system away from xenobiotics; this leads to increase in the efflux of compounds especially chemotherapeutic agents from the cells [42]. On the other hand, this protein is secreted in some tumor cells and leads to drug-resistant cancers [43, 44]. Therefore, it becomes imperative to know if a ligand serves as a substrate to P-gp (i.e., be conveyed out of the cell) or as an inhibitor (to weaken or damage the function of P-gp). All the thirteen studied ligands and standard drug Voxelotor are evaluated to be P-gp non substrate expect these ligands phenoxathiine (A8) and 2,4,6-trihydroxy-2-[(4-hydroxyphenyl) methyl]-1-benzofuran-3-one (A12). In metabolism, A3, A8, A10 and standard drug (Voxelotor) could serve as both non-substrate and inhibitors to CYP3A4, these ligands may cause increase in concentration and overdose of drugs while other compounds have no inhibitory effect on the CYP3A4 enzyme. This means they will have high chance of being converted and hence accessible after oral treatments. All the ligands with Voxelotor inclusive are non-substrate to CYP2D6 and CYP2C9. Ligands A1, A7, A13 and (Voxelotor) are inhibitors to CYP2D6; A3, A7, A10 and (Voxelotor) are inhibitors to CYP2C9 (Table 3); A11 and A12 are non-inhibitors to CYP1A2, and A7 could serve as both inhibitor and substrate to CY2C19 protein. Thus, M-coumaric acid (A11), 2,4,6-trihydroxy-2-[(4-hydroxyphenyl) methyl]-1-benzofuran-3-one (Maesopsin, A12) and Luteolin (A13) have superior metabolic properties than the standard drug [45].

Skin permeability (LogKp) is an important characteristic to be considered when evaluating medicines that may require transdermal delivery [46]. The predicted skin permeation log Kp is − 9.14 cm/s [38]. All the ligands have a lesser value compared to the recommended value, which means they all have good skin permeability. The synthetic accessibility values of the compounds were evaluated based on a scale ranging from 1 (easy to synthesize) and 10 (not easily to synthesis) and these values suggested that the ligands can be easily synthesized. Ligands A9 and A13 showed no pain alert while others has pain alert. Brain or Intestinal Estimate D permeation method (BOILED-Egg) is an intuitive method to predict simultaneously two key ADME parameters, the passive gastrointestinal absorption (HIA) and brain access BBB [38]. Points located in the BOILED-Egg's yellow represent the analogues predicted to passively permeate the BBB while points in the egg white are relative to the analogues predicted to face passive absorption by the gastrointestinal tract [47].This implies that compounds A1, A2, A3, A4, A5, A6, A7, A8, A9, A10, A11can access the brain while A12 and A13 have good gastrointestinal absorption (HIA). Pro-Tox II software predicted that ligands **A1, A2, A10, A11, A13** and Voxelotor could be classified as toxicity, with LD_{50} ranging from $2000 \leq LD_{50} \leq 5000$ mg/kg wich may be harmful if swallowed.

Table 2
Physiochemical analysis for ligands and the standard drug

	L	BS	MW	TPSA	LogPo/w	HD	HA	Syn	LD_{50}	PC	CY	Mu	I	H	C	Log S	AOT
A1	Yes	0.55	220.31	40.46	3.09	2	2	2.17	3200	5	In	In	In	In	In	-3.3	III
A2	Yes	0.55	194.23	46.30	1.79	3	1	1.52	2580	5	In	In	In	In	In	-1.8	III
A3	Yes	0.55	228.21	60.69	2.48	3	3	2.02	200	3	In	In	In	In	In	-3.6	III
A4	Yes	0.55	192.17	59.67	1.52	4	1	2.62	945	4	In	In	In	In	A	-2.4	III
A5	Yes	0.55	202.16	63.58	1.77	4	1	3.68	500	4	In	A	A	In	A	-2.7	II
A6	Yes	0.55	186.10	43.35	2.21	3	0	3.07	520	4	In	In	A	In	In	-2.9	II
A7	Yes	0.55	250.30	38.69	3.31	3	1	2.29	500	4	In	In	In	In	In	-4.0	III
A8	Yes	0.55	200.26	34.14	3.62	1	0	3.14	1100	4	In	In	In	In	In	-4.5	III
A9	Yes	0.55	208.21	34.14	2.46	2	0	2.33	2000	4	In	A	In	In	In	-3.2	III
A10	Yes	0.55	244.24	80.92	2.08	4	4	2.36	4000	5	In	In	In	In	In	-3.4	III
A11	Yes	0.85	104.16	57.3	1.36	3	2	1.74	2500	5	In	In	In	A	In	-2.2	III
A12	Yes	0.55	288.24	107.22	1.37	6	4	3.09	2000	4	In	In	In	In	In	-3.2	III
A13	Yes	0.55	286.24	111.13	1.73	6	4	3.09	3919	5	In	In	In	In	In	-3.7	III
SD	Yes	0.55	337.37	77.24	2.59	5	1	2.89	4540	5	In	A	In	In	A	-3.7	IV

L = Lipinski, BS = Bioactivity score, GI = Gastrointestinal tract Absorption, LogK = Skin permeamility, MW = molecular weight, SY = Synthetic accessibility, HA = No of hydrogen bond acceptor, HD = No of hydrogen bond donor, LogPo/w = partition coefficient, H = Hepatoxicity, C = Carcinogenicity, I = Immunotoxicity, Mu = Mutagenicity, Cy = Cytotoxocity, AOT = Acute Oral Toxicity, A = Active, In = Inactive

Table 3
ADMET profile of analysis for ligands and the standard drug

Lig	GI	BBB	CYP3A4 Inh	CYP3A4 Sub	CYP1A2 Inh	CYP1A2 Sub	CYP2C19 Inh	CYP2C19 Sub	CYP2C9 Inh	CYP2C9 Sub	CYP2D6 Inh	CYP2D6 Sub
A1	High	Yes	No	Yes	Yes	No	No	No	No	No	Yes	No
A2	High	Yes	No	No	Yes	Yes	No	Yes	No	No	No	No
A3	High	Yes	Yes	Yes	Yes	No	No	No	Yes	No	No	No
A4	High	Yes	No	No	Yes	Yes	No	No	No	No	No	No
A5	High	Yes	No	No	Yes	Yes	No	No	No	No	No	No
A6	High	Yes	No	No	Yes	Yes	No	No	No	No	No	No
A7	High	Yes	No	Yes	Yes	Yes	Yes	Yes	Yes	No	Yes	No
A8	High	Yes	Yes	Yes	Yes	Yes	Yes	No	No	No	No	No
A9	High	Yes	No	Yes	Yes	No	Yes	No	No	No	No	No
A10	High	No	Yes	Yes	Yes	No	No	Noz	Yes	No	No	No
A11	High	Yes	No	No	No	No	No	No	No	No	No	No
A12	High	No	No	No	No	No	No	No	No	No	No	No
A13	High	No	Yes	No	Yes	No	No	No	No	No	Yes	No
SD	High	Yes	Yes	Yes	Yes	No	Yes	No	Yes	No	Yes	No
Inh = Inhibitor and Sub = Substrate												

Molecular docking analysis

The docking simulations of the DFT optimized structures of the compounds were carried out against Crystal Structure of Carbonmonoxy Sickle Hemoglobin in R-State Conformation (PDB ID: 5E6E) and the conformation in each ligand-receptor complex with highest free energy of interactions was considered as best and most suitable conformation. A potential active drug is expected to have inhibitory values from 0.1 and 1.0μM and it should not be greater than 10nM [48]. The binding affinity/scoring energy ranged from − 6.1 to -9.1Kcal/mol and the Inhibition constant ranged from 0.25 to 33.60 (μM). The molecular docking results were showed on Table 4 and Table 5. Phenanthrene-5,6-dione (A9) had − 9.1 Kcal/mol, 2-(3,4-dihydroxyphenyl)-5,7-dihydroxychromen-4-one (A13) had − 8.9 Kcal/mol with the target protein (PDB ID: 5E6E) while the standard drug Voxelor had − 7.4Kcal/mol. Phenanthrene-5,6-dione (A9) had Pi-Sigma interaction with the protein (PDB ID: 5E6E) via LEU A: 101 and VAL A: 62. Pi- Alkyl interaction with the protein (PDB ID: 5E6E) via LEU A: 136 and ALA A : 65. Conventional hydrogen bond interaction with the protein (PDB ID: 5E6E) via HIS A: 86 as shown in the Fig. 2. 2-(3,4-dihydroxyphenyl)-5,7-dihydroxychromen-4-one (A13) had Pi-Sigma interaction with the protein (PDB ID: 5E6E) via VAL A: 62, Pi- Alkyl with LEU A: 66, VAL A : 132, ALA A: 65, and LEU A: 83, Pi-Sigma interaction with VAL A : 62, Van Der Waaals interaction with SER A : 102, HIS A:87, LEU A: 136, LYS A : 61 LEU A :105, conventional hydrogen bond interaction with PHE A: 98, LEU A: 129, SER A: 133 and unfavorable donor-donor interaction with HIS A: 58 (Fig. 2).

Table 4
Showing the binding affinity and non-bonding interactions of 5E6E receptor with the ligands

Ligand	Binding affinity ΔG (Kcal/mol)	Inhibition constant Ki (μM)
A1	-6.6	14.45
A2	-6.9	8.70
A3	-6.1	33.60
A4	-6.1	33.60
A5	-6.4	20.25
A6	-7.9	1.60
A7	-6.2	28.38
A8	-7.2	5.24
A9	-9.1	0.25
A10	-7.6	2.67
A11	-6.6	14.45
A12	-7.5	3.16
A13	-8.9	0.29
Voxelor	-7.4	3.74
Coligand (Protoporphyrin IX containing Fe)	-8.6	0.49

Table 5
Binding affinity and non-bonding interactions of 5E6E receptor with the ligands

IUPAC NAME	Binding affinity ΔG (kcal/mol)	Inhibition constant Ki (μM)	5E6E receptor amino acids forming H bond with ligands	H-bond distance (Å)	Electrostatic / Hydrophobic interactions involved
furo[2,3-h]chromen-2-one (A6)	-7.9	1.60			
Phenoxathiine (A8)	-7.2	5.24			
phenanthrene-5,6-dione (A9)	-9.1	0.25	HIS A 87		LEU A: 101,LEU A: 136, ALA A ;65, Val A: 62, HIS A 87
4-[(E)-2-(3,5-dihydroxyphenyl)ethenyl]benzene-1,3-diol (A10)	-7.6	2.67			PHE A: 43, TYB A: 42, VAL A: 93, LEU A: 101,
2-(3,4-dihydroxyphenyl)-5,7-dihydroxychromen-4-one (A13)	-8.9	0.29	PHE A: 98, LEU a: 129, SER A: 133,	2.45, 1.93	HIS A: 58, LEU A: 66, PHE A: 98, LEU A: 129, SER A: 133, ALA A: 65, LEU A: 83 VAL A : 132, VAL A: 62 LEUA 136 LEUA 101 HIS A 87

Geometries of Calculated Molecular Description of the Studied Ligands

The thirteen phytochemicals (A1-A13) with good ADMET properties and Voxelotor (GBT-440) were optimized using Density Functional Theory (DFT) at ground state in water to calculate the reactivity descriptor of the compounds. The Density Functional Theory (DFT) of Beckes's three-parameter hybrid functional using the Lee, Yang and Parr correlation functional (B3LYP) [25, 26] with 6–31G (d,p) basis set was used for the geometry optimization and energy calculation. The calculated molecular descriptions are the highest occupied molecular orbital (HOMO), the

lowest unoccupied molecular orbital (LUMO), dipole moment (DM), Band Gap ($E_g = E_{HOMO} - E_{LUMO}$), electron affinity (EA = - E_{LUMO}), ionization potential (IP = - E_{HOMO}), Chemical potential (μ = $\frac{IP+EA}{2}$), chemical hardness (η = $\frac{IP-EA}{2}$), chemical softness (S $= 1/2\eta$), electron donating power ($\omega^- = \frac{(3IP+EA)^2}{16(IP-EA)}$), electron accepting power ($\omega^+ = \frac{(IP+3EA))^2}{16(IP-EA)}$), global electrophilicity index (⍰ = $\frac{(IP+EA)^2}{4(IP-EA)}$) and $\Delta\omega^{\mp}$ $(\omega^+ - \omega^-)$ as presented in Table 6. The frontier orbital energies (the HOMO and LUMO) govern chemical reactivity of a molecule in which the HOMO and LUMO denoting electron donating and accepting capability, respectively, of a molecule. Thus, the high value of HOMO energies enhances the ligand's capacity bind with receptor [49]. The HOMO and IP energies show that **A13** can easily release electrons to the surrounding receptor and also exhibits strong interactions than the **A9** and standard drug (Voxelotor (GBT-440). Also, μ, ω, $\Delta\omega^{\mp}$ and dipole moment values as shown in Table 6 support stronger stability of **A13** in the protein-ligand complex, stronger electron accepting capability and stronger non-bonding interactions between the ligand and protein. The MEP diagram shows that 2-(3,4-dihydroxyphenyl)-5,7-dihydroxychromen-4-one (**A13)** about four nucleophilic centers on hydroxyl oxygen atoms which may enhance its interactions with the receptor (Fig. 3). The HOMO, IP, ω and $\Delta\omega^{\mp}$ values suggested that **A9** and the standard drug may have similar energetic interactions with the protein, which is agreement with the calculated docking affinity.

Table 6
Optimization of the ligands and drugs in water

COMP	HOMO eV	LUMO eV	DM Debye	Eg	μ	η	IP	EA	ω	$\Delta\omega^{\mp}$
A1	-5.68	-0.04	2.35	5.64	-2.86	2.82	5.68	0.04	1.44	-3.60
A2	-5.50	-0.28	3.63	5.22	-2.89	2.61	5.50	0.28	1.59	-3.85
A3	-5.31	-1.28	2.88	4.03	-3.29	2.02	5.31	1.28	2.68	-5.89
A4	-5.68	-1.58	9.78	4.10	-3.63	2.05	5.68	1.58	3.21	-6.95
A5	-5.79	-1.56	7.04	4.23	-3.67	2.12	5.79	1.56	3.17	-6.91
A6	-6.12	-1.49	5.27	4.63	-3.80	2.32	6.12	1.49	3.11	-6.83
A7	-5.42	-1.07	0.18	4.35	-3.25	2.18	5.42	1.07	2.42	-5.39
A8	-5.57	-0.49	1.43	5.08	-3.03	2.54	5.57	0.49	1.80	-4.25
A9	-6.26	-2.69	5.98	3.57	-2.48	1.79	6.26	2.69	1.72	-4.37
A10	-5.38	-1.28	1.69	4.10	-3.33	2.05	5.38	1.28	2.70	-5.92
A11	-6.11	-1.65	4.03	4.46	-3.88	2.23	6.11	1.65	3.37	-7.30
A12	-5.84	-1.58	3.07	4.26	-3.71	2.13	5.84	1.58	3.08	6.99
A13	-5.74	-1.65	6.28	4.09	-3.69	2.05	5.74	1.65	3.30	-7.19
Voxelotor	-6.48	-0.08	3.60	6.40	-3.28	3.2	6.48	0.08	1.60	-4.16

Molecular dynamic simulation (MDS)

The molecular docking analysis supported by DFT results was further investigated by performing molecular dynamic simulation study. This is done to predict the actual binding stabilities between ligands phenanthrene-5,6-dione (A9), 2-(3,4-dihydroxyphenyl)-5,7-dihydroxychromen-4-one (A13) and the standard drug) and Carbonmonoxy Sickle Hemoglobin in R-State Conformation (PDB ID: 5E6E). Molecular dynamic simulation study was done to understand the positions of different atoms and molecules during the binding of the ligands with the receptors [50]. Furthermore, 100ns MDS experimentation observed parameters like Solvent Accessible surface area, RMSD, and free energy binding component plot interpretation, revealed deviation and fluctuation of **5E6E** during the simulation. The root mean square deviation (RMSD) provides a measure of the average distance between the atoms of the protein–ligand complexes. The RMSD values were in the range of 0.1–2.3 nm throughout the period for all complexes [51]. The 5E6E complexation with 2-(3,4-dihydroxyphenyl)-5,7-dihydroxychromen-4-one **(A13)**, showed a stable pattern as compared to that of phenanthrene-5,6-dione **(A9)** (Fig. 4). The observed RMSD values for phenanthrene-5,6-dione **(A9)**, 2-(3,4-dihydroxyphenyl)-5,7-dihydroxychromen-4-one (A13) and standard drug Voxelotor (GBT-440) complexed with **5E6E** were between 0.12 and 0.17 nm and gained more stability from 0 to 100 ns as showed on Fig. 5. Van der Waals calculations, electrostatic potential energy and polar solvation, of the ligands phenanthrene-5,6-dione **(A9)**, 2-(3,4-dihydroxyphenyl)-5,7-dihydroxychromen-4-one2-(3,4-dihydroxyphenyl)-5,7-dihydroxychromen-4-one **(A13)** and voxelotor with the target (PDB: 5E6E) were shown in the Table 7 and on Fig. 6.

Table 7
Decomposition of free energy components for 5E6E

Lig	VDWAALS	EEL	EPB	ENPOLAR	GGAS	GSOLV	TOTAL
A9	-31.61 ± 0.03	-4.36 ± 0.06	24.88 ± 0.05	-2.69 ± 0.00	-35.96 ± 0.06	22.18 ± 0.05	-13.78 ± 0.05
A13	-34.09 ± 0.04	-7.62 ± 0.08	34.73 ± 0.08	-3.58 ± 0.00	-41.71 ± 0.09	31.15 ± 0.08	-10.56 ± 0.07
Voxelotor	-45.01 ± 0.05	-4.42 ± 0.06	29 ± 0.06	-4.2 ± 0.00	-49.43 ± 0.08	24.8 ± 0.06	-24.63 ± 0.07

Conclusion

A conventional or traditional clinical trial method takes a significant expenditure in time, money and resources, and it is also possible that such drug candidate fails. Molecules which involves in the clinical trials such as chemical entity, orphan molecule and drug candidates need to undergo in silico modelling in order to confirm the physiochemical properties, drug-ability and their atomicity level. In this study, twenty six (26) potential compounds for managing sickle cell disease were evaluated for their drug-likeness in treating sickle cell disease using PASS, ADMET, DFT Molecular docking and Molecular dynamic simulation. Phenanthrene-5,6-dione **(A9)** was reported to be found in *Moringa lucida*, a plant that has efficacy in treating sickle cell diseases. 2-(3,4-dihydroxyphenyl)-5,7-dihydroxychromen-4-one **(A13, Luteolin)** is a phytochemical found in *Cajanus Cajan* seeds, this plant was reported in the literature to possess anti-sickling properties. *Cajanus Cajan* was reported to assist in reduction of polymerization rate, reverse sickle red blood cell, increase the oxygen affinity of Hb. The results obtained from the in silico analysis showed that compounds phenanthrene-5,6-dione **(A9)** and 2-(3,4-dihydroxyphenyl)-5,7-dihydroxychromen-4-one **(A13, Luteolin)** has higher potential in treating sickle cell disease than the standard drug voxelotor (GBT-440). 2-(3,4-dihydroxyphenyl)-5,7-dihydroxychromen-4-one is a flavonoid and a rutin phytochemical and phenanthrene-5,6-dione (A9) is an anthraquinone. Further research can be done on the derivatives of these compounds.

Declarations

Funding

No funding received for this work

Acknowledgments

The Authors acknowledged the Department of Pure and Applied Chemistry, Ladoke Akintola University of Technology for the computational facilities.

Availability of Data and Material Statement: All data generated or analyzed during this study are included in this article.

Authors contribution

Yemisi Elizabeth Asibor:Conceptualization and writing of original manuscript, Banjo SEMIRE: Supervisor, review, and editing of the manuscript, Abel Kolawole OYEBAMIJI**:** Data curation, Dayo Felix LATONA**:** Editing and review,

Conflicts of Interest

There is no conflict of interest regarding the publication of this article.

References

1. Olubiyi, O.O., Olagunju, M.O, Strodel, B., 2019. Rational Drug Design of Peptide-Based Therapies for Sickle Cell Disease. Molecules. 12;24(24):4551.https://doi.org/10.3390/molecules24244551.
2. Martin, C.R., Cobb, C., Tatter, D., Johnson, C., Haywood, L. J., 1983. Acute myocardial infarction in sickle cell anemia. Arch Intern Med. Apr;143(4):830–1. PMID: 6838304.
3. Araujo, M. D. (2019). Anemia falciforme complicada por crise vaso-oclusisındrome toracica aguda.UNIFACIG Scientific Seminar. Manhuac¸
4. Martins, P. J., Moraes-Souza, H., & Silveira, T. B. (2010). Morbimortalidade em doenc¸a falciforme. Revista Brasileira de Hematologia e Hemoterapia, 32(5), 378–383. https://doi.org/10.1590/S1516-84842010000500010.
5. Aldallal S M, 2020. Voxelotor: A Ray of Hope for Sickle Disease. Cureus 12(2):.https://doi.org/10.7759/cureus.7105

6. Levien, T.L., Baker D.E., 2020. Crizanlizumab. Hosp Pharm. 2023;58(1):23–29. doi: 10.1177/0018578720925373. Epub 2020 Jun 6. PMID: 36644753; PMCID: PMC9837322.
7. Harborne, J.B. (1973). Phytochemical Methods. Chapman and Hall Ltd., London, 49–188.https://doi.org/10.4236/jgis.2023.151002
8. Okwu, D.E. (2004) Phytochemical and Vitamin Content of Indigenous Species of South-Eastern Nigeria. Journal of Agriculture and the Environment, 6, 30–37.https://doi.org/10.4236/nr.2021.128016
9. Okwu, D.E. (2005). Phytochemicals, vitamins and mineral contents of two Nigerian medicinal plants. *InternationJournal of Molecular Medicine and Advance Sciences*,1(4): 375 – 38.10.12691/ajbr-6-1-1.
10. Sofowora, A. (1993). Medicinal Plants and Traditional Medicine in Africa. Spectrum Books Ltd., Ibadan, 191–289.https://doi.org/10.4236/pp.2023.1410027
11. Fulata, A. M Hamidu U, Muhammad A. T, A D, AlhajiBukar U A. Busuguma, B M. Kagu 2023. Phytochemical Evaluations, In-vitro Anti-sickling and Polymerization Inhibition Potentialsof the Crude Methanol Leaf Extracts of Carica papaya LINN. and Psidumguajava LINN.Nigerian Journal of Pharmaceutical and Biomedical ResearchVol. 7 Issue.1 August, 2023. p-ISSN: 2579 – 1419 e-ISSN: 2814 – 1415.http://www.unn.edu.ng/nigerian-research-journal-of-chemical-sciences/
12. Ameh, O. O. Obodozie, B. A. Chindo, P. C. Babalola, and K. S. Gamaniel, 2012. "Herbal clinical trials—historical development and application in the 21st Century," Pharmacologia, vol. 3, pp. 121–131.https://doi.org/10.1155/2012/607436
13. Ameh, O. O. Obodozie, P. C. Babalola, and K. S. Gamaniel, 2011. "Medical herbalism and herbal clinical research—a global perspective," British Journal ofPharmaceutical Research, vol. 1, no. 4, pp. 99–123,
14. Ngbolua KN, Mpiana PT. 2014. The Possible Role of a Congolese polyherbal formula (Drepanoalpha®) as source of Epigenetic Modulators in Sickle Cell Disease: A Hypothesis J. *of Advancement in Medical and Life Sciences*. V2I1. DOI: 10.15297/JALS.V2I1.02.
15. Iyamu, E.W., Turner, E.A., Asakura, T., 2002. In vitro effects of NIPRISAN (Nix-0699): a naturally occurring, potent antisickling agent. British Journal of Haematology, Volume 118, Issue 1, pages 337–343.https://doi.org/10.1046/j.1365-2141.2002.03593.x
16. Chakraborty, D., Chattaraj, P.K 2021. Conceptual Density Functional Theory Based Electronic Structure Principles. Chem. Sci. *12*, 6264–6279.https://doi.org/10.1039/D0SC07017C
17. Heidar-Zadeh, F., Ayers, P.W., Carbó-Dorca, R 2018. A Statistical Perspective on Molecular Similarity. In *Conceptual Density Functional Theory and Its Application in the Chemical Domain*; Islam, N., Kaya, S., Eds.; Apple Academic Press: Toronto, ON, Canada,; Chap. 10, pp. 263–273.
18. Geerlings, P., Chamorro, E., Chattaraj, P.K., De Proft, F., Gázquez, J.L., Liu, S., Morell, C.; Toro-Labbé, A.; Vela, A.; Ayers, P 2020,. Conceptual Density Functional Theory: Status, Prospects, Issues. Theor. Chem. Acc. *139*, 36.
19. Poater, A., Saliner, A.G., Solá, M., Cavallo, L., Worth, A.P 2010. Computational Methods to Predict the Reactivity of Nanoparticles Through Structure-Property Relationships. Expert Opin. Drug Deliv. *7*, 295–305.
20. Ayers, P., Parr, R. 2000. The Variational Principles for Describing Chemical Reactions: The Fukui Function and Chemical Hardness Revisited. J. Am. Chem. Soc. *122*, 2010–2018. [CrossRef].https://doi.org/10.1517/17425240903508756
21. Lagunin A, Stepanchikova A, Filimonov D, Poroikov V (2000). PASS: Prediction of Activity Spectra for Biologically Active Substances. Bioinformatics 16(8):747–748. https://doi.org/10.1093/bioinforma tics/16.8.747.https://doi.org/10.1021/ja9924039
22. Yang, H., Lou, C., Sun, L., Li, J., Cai, Y., Wang, Z., Li, W., Liu, G. and Tang,Y. (2019). admetSAR 2.0: web-service for prediction and optimization of chemical ADMET properties. Bioinformatics, 35,1067–1069.https://doi.org/10.1093/bioinformatics/bty707
23. Cheng,F., Weihua, L, Yadi, Z., Jie, S., Zengrui, W., Guixia, L., Philip W. Lee, Yun, T.,. admetSAR: (2012). A comprehensive source and free tool for evaluating chemical ADMET properties. J. Chem. Inf. Model., 52(11): 3099–3105. https://doi.org/10.1021/ci300367a
24. Egan, W.J., Merz, K.M., Baldwin, J.J., (2000). Prediction of drug absorption using multivariate statistics. J Med Chem 43(21):3867–3877.https://doi.org/10.1021/jm000292e
25. Becke, A.D., (1993). Density-functional thermochemistry. III. The role of exact exchange. J. Chem. Phys. 98: 5648–565. https://doi.org/10.1063/1.464913
26. Lee, C., Yang, W., Parr, R.G (1988). Development of the Colle-Salvetti correlation-energy formula into a functional of the electron density. Phys. Rev. B 37: 785–789.https://doi.org/10.1103/PhysRevB.37.785
27. Jacquemin, D., Perpete, E.A., Ciofini, I., Adamo, C. 2008. Accurate simulation of optical properties in dyes, Accounts of chemical Research;42:326–3344.https://doi.org/10.1021/ar800163d
28. Safo, Ghatge, M.S., Ahmed, M.H., Omar, A.S., Pagare, P.P., Rosef, S., Kellogg, G.E., Abdulmalik,O.,,(2016). M.K. J Struct Biol 194: 446–450. https://doi.org/10.1016/j.jsb.2016.04.003.
29. Tian, W., Chang, C.,, Xue, L., Jielin, Z.,, Jie, L., CASTp 3.0: computed atlas of surface topography of proteins, *Nucleic Acids Research*, Volume 46, Issue W1, 2 July 2018, Pages W363–W367, https://doi.org/10.1093/nar/gky473
30. Tian, W., Chen, C., Lei, X ., (2019). CASTp 3.0: computed atlas of surface topography of proteins. Nucleic Acids Res 46: W363–W367.

31. Van Der Spoel, D., Lindahl, E., Hess, B.,Groenhof, G., Mark, A.E., Berendsen, H.J., 2005. GROMAC. Fast, Flexible and free. J computaion Chemistry 26 (16), 1701–1701.https://doi.org/10.1002/jcc.20291
32. Zoete, V., Cunendet, M. A., Grosdidier, A., Michielin, O., (2011). SwissParam: a fast forcefield generation tool for small organic molecules. J computaion Chemistry 32 (11), 2359–2368.
33. Jamal, M.S., Alharbi, A. H., Ahmad, V., (2021). Identification of dexorubicin as a potential therapeutic against SARS-CoV-2 (COVID 19) protease: a molecular docking and dynamics simulation studies. J. Biomolecular Structure Dyn. 1–15.https://doi.org/10.1080/07391102.2021.1905551
34. Gupta, K., Gupta, P., Solovey, A., Hebbel, R.P., (1999). Mechanism of interaction of thrombospondin with human endothelium and inhibition of sickle erythrocyte adhesion to human endothelial cells by heparin. Biochemistry. Biophysics. Acta. 1453:63–73.https://doi.org/10.1016/S0925-4439(98)00085-4
35. Kufareva, I., Abagyan, R., 2012. Methods of protein structure comparison. Method Molecualr 857,231–257.https://doi.org/10.1007/978-1-61779-588-6_10
36. Kuzamanic, A., Zagrovic, B., 2010. Determination of ensemble-average pairwise root mean-square deviation from experimental B-factors Biophysics. J. 98 (5), 861–871.https://doi.org/10.1016/j.bpj.2009.11.011
37. Turner, P., 2005, XMGRACE Version 5.1.19. Center for coastal and Land-Margin Research, Oregon Graduate Institute of Science and Technology, Beaverton. Daina, A., Zoete, V., (2017). SwissADME: a free web tool to evaluate pharmacokinetics, drug likeness and medicinal chemistry friendliness of small molecules. Sci Rep,; 7:1 – 13.https://doi.org/10.1038/srep42717
38. Lipinski, C.A., Lombardo, F., Dominy, B.W., Feeney, P.J. (2001). Experimental and computational approaches to estimate solubility and permeability in drug discovery and development settings. Advances in Drug Delivery. Revision., *46*, (1–3), 3–26.https://doi.org//10.1016/s0169-409x(00)00129-0
39. Lipinski, C. A., (2004). "Lead-and drug-like compounds: the rule-of-five revolution." Drug Discovery Today: Technologies 1.4: 337–3. https://doi.org/10.5772/52642
40. Veszelka, S., Tóth, A., Walter, F.R., Tóth, A.E., Gróf, I., Mészáros, M., Bocsik, A., Hellinger, É., Vastag, M., Rákhely, G., (2018). Comparison of a Rat Primary Cell-Based Blood-Brain Barrier Model with Epithelial and Brain Endothelial Cell Lines: Gene Expression and Drug Transport. Front. Mol. Neurosci., 11, 166. [CrossRef] [PubMed] doi: 10.3389/fnmol.2018.00166. eCollection 2018.
41. Adegbola, P.I., Semire, B., Fadahunsi, O.S. and Adegoke, A.E., (2021). Molecular docking and ADMET studies of Allium cepa, Azadirachta indica and Xylopia aethiopica isolates as potential anti-viral drugs for Covid-19. VirusDisease. https://doi.org/10.1007/s13337-021-00682-7
42. Ukibayev, J., Datkhayev, U., Myrzakozha, D., Frantsev, A., Karlova, E., Nechepurenko, Y., Balpanova, D., & Almabekova, A. (2021). Rectal methods of delivery of medical drugs with a protein nature in the therapies of tumor disease. Journal of Advanced Pharmacy Education & Research, 11(1), 18–22. https://doi.org/10.51847/vcTFlpY
43. Lalthanpuii, K., Kaur, J., Saini, S., Bhatti, K., & Nain, P. (2022). Strengthen the Monitoring and Reporting of Adverse Drug Reaction at a Tertiary Teaching Hospital. Archives of Pharmacy Practice, 13(1), 61–67.https://doi.org/10.51847/Zq3HaDzGqf
44. Adegbola P.I., Fadahunsi, O.S., Ogunjinmi, O.E., Adegoke, A.E., Ojeniyi, F.D., Adesanya, A., Olagoke, E., Adisa, A.D., Ehigie, A.F., Adetutu, A., Semire B., (2023). Potential inhibitory properties of structurally modified quercetin/isohamnetin glucosides against SARS-CoV-2 Mpro; molecular docking and dynamics simulation strategies, Informatics in Medicine Unlocked 37, 101167, https://doi.org/10.1016/j.imu.2023.101167.
45. Khalfaoui, A., Noumi, E., Belaabed, S., Aouadi, K., 2021. LC-ESI/MS-phytochemical profiling with antioxidant, antibacterial, antifungal, antiviral and in silico pharmacological properties of Algerian Asphodelus tenuifolius (Cav.) organic extracts. Antioxidant. April. 10. 628. doi.org/10.3390/antiox10040628.
46. Al Azzam, K.M., Negim, E. S., Aboul-Enein, H. Y., 2020. ADME studies of TUG-770 (a GPR-40 inhibitor agonist) for the treatment of type 2 diabetes using SwissADME predictor: *In* silico study.J Appl Pharm Sci, 12(04):159–169.DOI: 10.7324/JAPS.2022.120418
47. Olajide, M., Abdul-Hammed, M., Bello, I. A., Adedotun, I. O., and Afolabi, T. I.,. "Identification of potential inhibitors of thymidylate synthase (TS) (PDB ID: 6QXH) and nuclear factor kappa-B (NF–κB) (PDB ID: 1A3Q) from *Capsicum annuum* (bell pepper) towards the development of new therapeutic drugs against colorectal cancer (CRC)" Physical Sciences Reviews, 2023. https://doi.org/10.1515/psr-2022-0281
48. Oyebamiji, A. K., Olujinmi F. E., Akintelu, S. A., Adetuyi, B., Ogunlana, O., Semire, B., Akintayo, E. T., Akintayo, C. O., Babalola, J. O., Olawoye, B. M., Aworinde, J. O., (2024). Predicting the biological activity of selected phytochemicals in Alsophila spinulosa leaves against 4-aminobutyrate-aminotransferase: A potential antiepilepsy agents. Eclet. Quim. 49 e-1492 https://doi.org/10.26850/1678-4618.eq.v49.2024.e1492
49. De Vivo, M., Masetti, M., Bottegoni, G., Cavalli, A. (2016). Role of Molecular Dynamics and Related Methods in Drug Discovery. J. Med. Chem., *59*, 4035–4061.https://doi.org/10.1021/acs.jmedchem.5b01684

50. Malik, S.1., Shaikh, F., Meshari, A., Alsharif, I., Qazi, M. S. J., Jabir, H., Al-Fahemi, Amrita B., A., C., Samir, P., Ahmed K.I., and Saleh A. A., (2022). Antibacterial Properties and Computational Insights of Potent Novel Linezolid-Based Oxazolidinones.

Figures

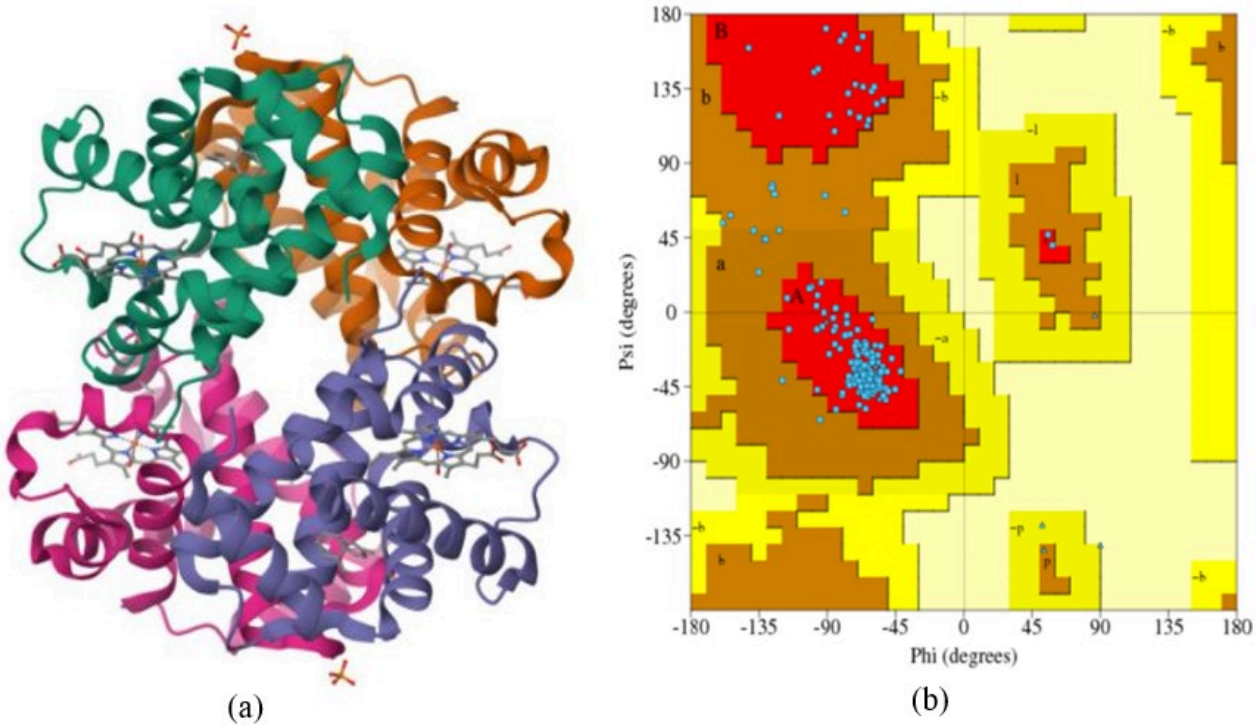

Figure 1

(a) crystal structure and binding pocket of Carbonmonoxy Sickle Hemoglobin in R-State Conformation (PDB ID: 5E6E) and (b) Ramachandran plot.

CODE	2D Binding Interactions	Binding Surface	3D Binding Interactions
A9	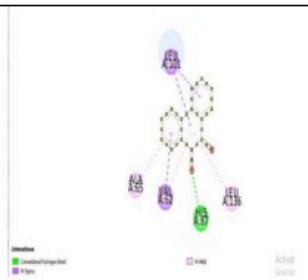	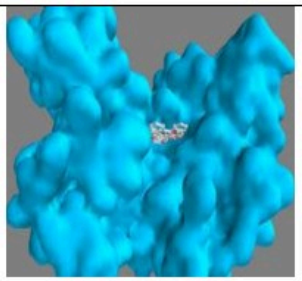	
A13	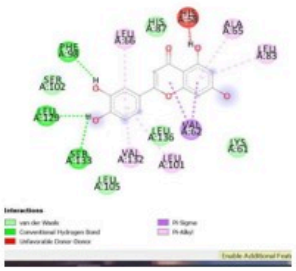	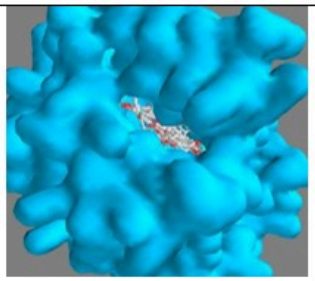	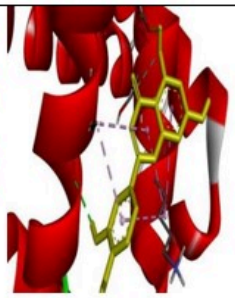

Figure 2:

Figure 2

Legend not included with this version

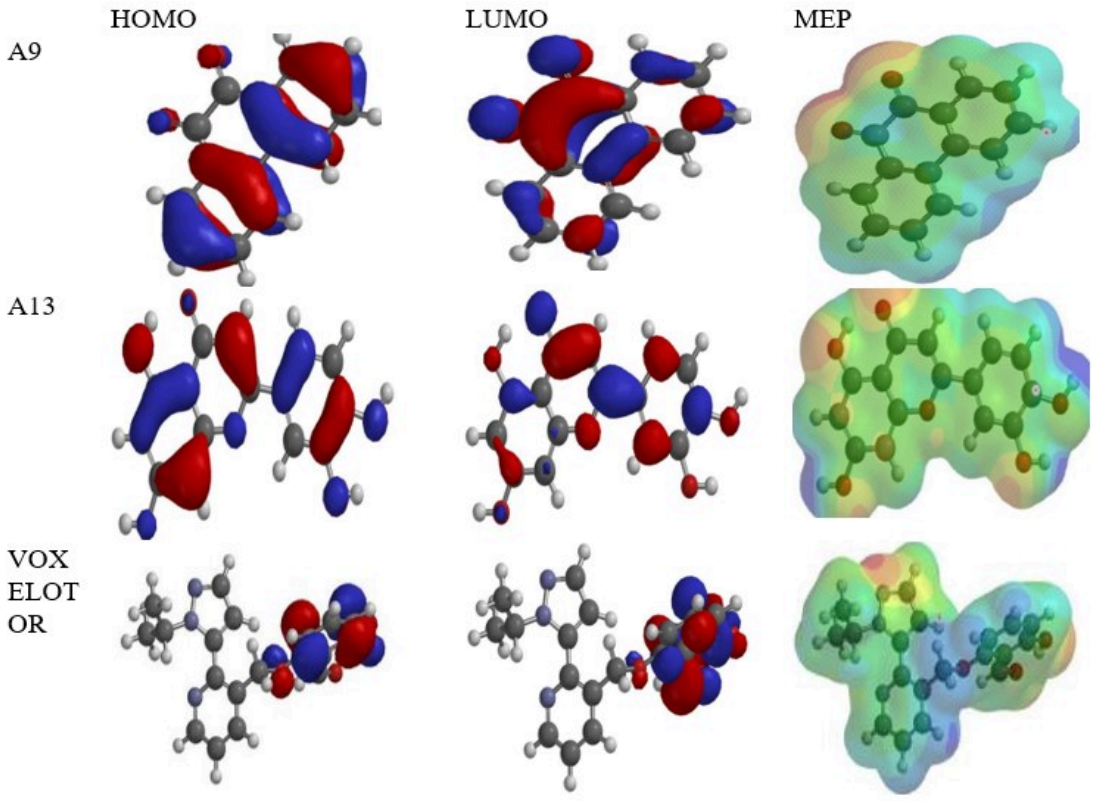

Figure 3

The frontier orbitals and molecular electrostatic potential (MEP) diagrams for A9, A13 and Voxelotor (GBT-440)

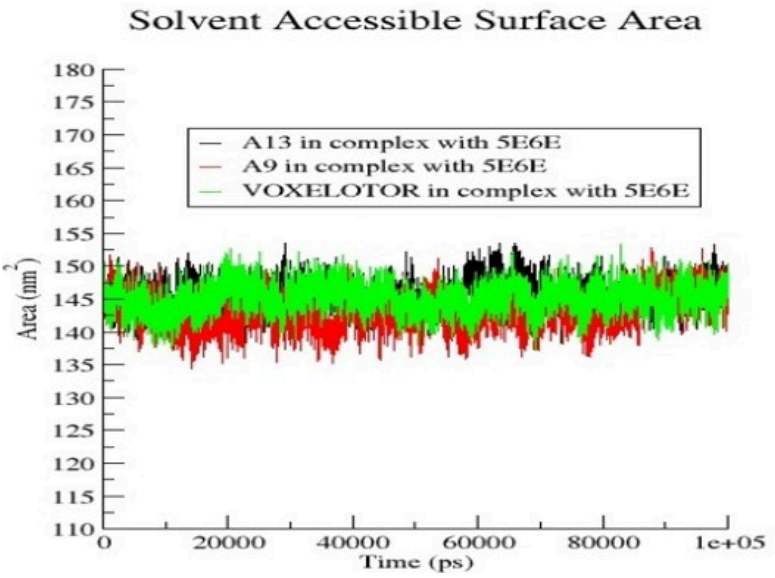

Figure 4

Solvent accessible surface area plot of phenanthrene-5,6-dione (A9), 2-(3,4-dihydroxyphenyl)-5,7-dihydroxychromen-4-one (A13), and Voxelotor with 5E6E.

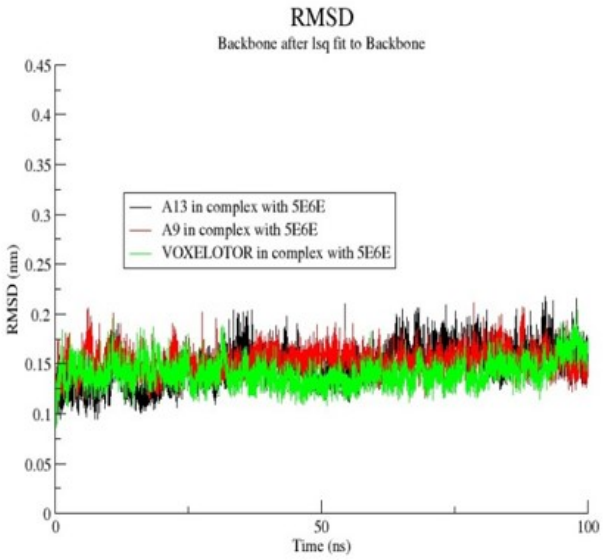

Figure 5

Graphical representation showing RMSD plot of phenanthrene-5,6-dione (A9), 2-(3,4-dihydroxyphenyl)-5,7-dihydroxychromen-4-one (A13), and Voxelotor with 5E6E

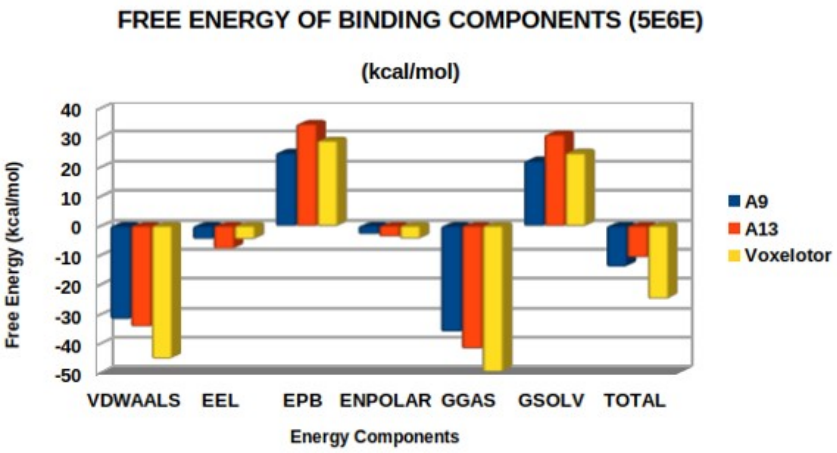

Figure 6

Free energy of binding components plot of phenanthrene-5,6-dione (A9), 2-(3,4-dihydroxyphenyl)-5,7-dihydroxychromen-4-one (A13), and Voxelotor with 5E6E.